Supporting information

Water oxidation kinetics of nanoporous $BiVO_4$ photoanodes functionalised by nickel/iron oxyhydroxide electrocatalysts

Laia Francàs,[1ǂ] Shababa Selim,[1ǂ] Sacha Corby,[1] Dongho Lee,[2] Camilo A. Mesa,[1] Ernest Pastor,[1] Kyoung-Shin Choi,[2] James R. Durrant[1]*

1. Department of Chemistry, Imperial College London, White City Campus, London W12 0BZ, United Kingdom
2. Department of Chemistry, University of Wisconsin-Madison, Madison, Wisconsin 53706, United States

[ǂ]Authors contributed equally.

Table of Contents

Section	Page Number
Experimental Details	S2
A. Electrocatalyst activation process	S5
B. SEC: Spectra of MOOH(++) species under electrochemical water oxidation	S6
C. NiOOH deactivation	S7
D. Extinction coefficient estimation	S8
E. Transient absorption spectroscopy	S10
F. Stability of $BiVO_4$/Ni(Fe)OOH photoanodes	S11
G. TOF (s^{-1}) and τ (s) calculation from measured [++] state densities and electrochemically measured water oxidation current densities	S11
References	S11

Experimental Details

a. Electrocatalysts Preparation:

The experimental procedure for the preparation of FeOOH, Ni(Fe)OOH and FeOOHNiOOH electrocatalysts deposited on FTO have been detailed previously.[S1] We note that the thickness of FeOOH on FTO used in this study (~ 80nm) is significantly thinner than that in our previous work (~350 nm), while those of Ni(Fe)OOH are comparable in both studies.[S2] As the electrical conductivity of FeOOH is low,[S3] the thickness of FeOOH can considerably affect the electrocatalytic properties of FeOOH. This is why the performance of Ni(Fe)OOH was better than that of the thicker FeOOH in our previous study[S2] while the performance of the thinner FeOOH in this study is comparable to that of Ni(Fe)OOH. Significant mixing of the FeOOH and NiOOH layers are observed in the as-prepared FeOOHNiOOH films studied herein, where a substantial proportion of the Ni is deposited within the voids of the FeOOH layer.[S1]The catalyst loading for our three electrocatalyst films studied herein have been previously determined using ICP-OES analysis,[S1] and tabulated below.

Table S1. Catalyst loading of the as-prepared Ni(Fe)OOH, FeOOH and FeOOHNi(Fe)OOH films.

Samples	Fe content (10^{-8} mol cm^{-2})	Ni content (10^{-8} mol cm^{-2})	Fe at. %
FeOOH	23.50	0.10	100
Ni(Fe)OOH	0.05	4.63	1
FeOOHNi(Fe)OOH	23.55	6.22	79

Impedance analyses of all three samples show that they have similar series resistance voltage losses (R_s ~ 33-44 Ohms) and therefore assigned mainly to FTO sheet resistance. Due to the similarity in the values obtained for the three electrocatalysts, we note that the J-V characteristics presented in this work are not iR corrected. Further, the main analysis for comparisons between electrocatalysts and photoanodes are *vs.* accumulated state density thus avoiding differences induced by differences in resistivities (at different thicknesses). In addition, data trends presented herein are also observed after iR correction.

b. Photoanodes preparation

$BiVO_4$ film preparation: The nanoporous $BiVO_4$ electrodes used in this study were based on the previously reported method with only one modification,[S2] which is the decrease in charge passed during the deposition of BiOI (from 0.13 C/cm^2 to 0.06 C/ cm^2). This is to prepare thinner $BiVO_4$ electrodes (from ~700 nm to 450-500 nm) that are transparent enough for the spectroscopic methods used in this study. The lateral dimensions of the $BiVO_4$ electrodes prepared in this study were 1 × 1.2 cm.

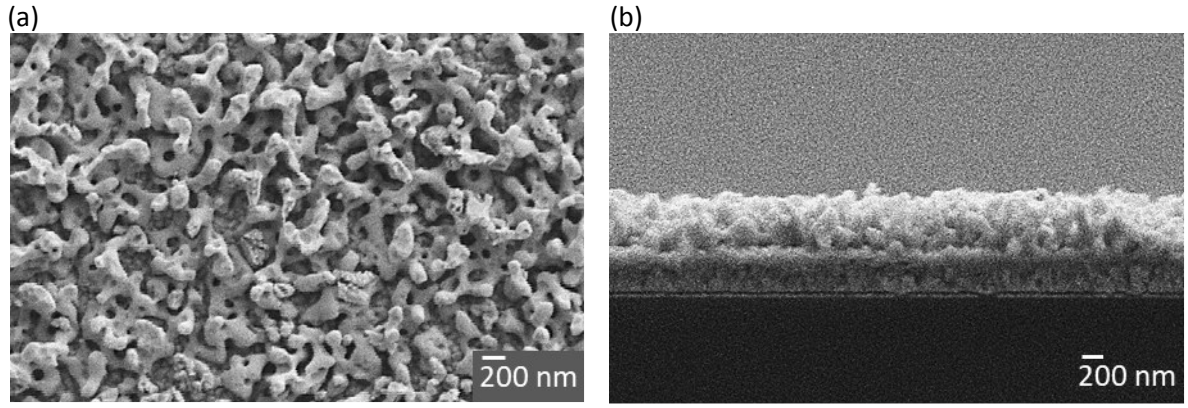

Figure S1. SEM images of nanoporous $BiVO_4$ films used in this study, of film thickness ~450-500 nm.

(a) Top view and (b) side view. Scale bars represent 200 nm.

Photodeposition of catalysts: The mechanisms of FeOOH and NiOOH photodeposition were reported previously.[2] A 0.1 M $FeSO_4 \cdot 7H_2O$ (Sigma-Aldrich, 99%) aqueous solution (pH ~ 4.3 as prepared and N_2 purged for 30 min before deposition) and a 0.1 M $NiSO_4 \cdot 6H_2O$ (Sigma-Aldrich, 98%) aqueous solution (pH adjusted to 6.8−7.0 using a 0.070 M NaOH (Sigma Aldrich, 97%) aqueous solution) were used for FeOOH and NiOOH photodeposition on $BiVO_4$ electrodes, respectively. Photodeposition was conducted in an undivided three-electrode cell using $BiVO_4$ electrode as the WE, Ag/AgCl (4 M KCl) as the RE and a platinum CE. A 300 W Xe arc lamp (Ushio, UXL-302-O) with an AM 1.5G filter was used as the light source. The light was back-illuminated on the $BiVO_4$ WE and the intensity was set to 1 mW/cm^2. For FeOOH photodeposition on $BiVO_4$, a constant potential of 0.23 V vs Ag/AgCl (4 M KCl) was applied to pass 30 mC/cm^2 with gentle stirring. For NiOOH photodeposition on $BiVO_4$, an open circuit potential of the $BiVO_4$ electrode in dark (ca. 0 V vs Ag/AgCl (4 M KCl)) was applied to pass 28.6 mC/cm^2 with gentle stirring. The resulting $BiVO_4$/FeOOH and $BiVO_4$/Ni(Fe)OOH films were rinsed with DI water and dried with a gentle stream of air. In order to prepare $BiVO_4$/FeOOHNiOOH electrode, photodeposition of NiOOH was carried out on the $BiVO_4$/FeOOH film using the same conditions described above. A total charge of 30 mC/cm^2 and 28.6 mC/cm^2 were passed for the FeOOH and NiOOH deposition, respectively. When depositing FeOOH and NiOOH on $BiVO_4$ in a row, $BiVO_4$/FeOOH was dried in air for at least 3 h before NiOOH photodeposition. Finally, the resulting $BiVO_4$/FeOOHNiOOH films were rinsed with DI water and dried with a gentle stream of air. The samples were transparently masked to give an exposed sample area between 0.13 – 0.2 cm^2.

The roughness factor of the thin, nanoporous $BiVO_4$ film used in this study was determined to be 20 based on the mass of $BiVO_4$ contained in the thin film and the specific surface area of nanoporous $BiVO_4$ (31.8 m^2/g) reported in our previous study.[S2] Using the roughness factor of $BiVO_4$ and the estimated amount of catalyst deposited (assuming 100% Faradaic efficiency of the charge passed during photodeposition), the thicknesses of FeOOH, Ni(Fe)OOH, and FeOOHNiOOH catalyst layers on the nanoporous $BiVO_4$ electrode were calculated to be 3 nm, 4 nm, and 7 nm, respectively. Our previous study confirmed that the addition of the catalyst layers on $BiVO_4$ does not affect the carrier density or depletion width of $BiVO_4$ by comparing the slopes of the Mott-Schottky plots of $BiVO_4$ with and without the catalyst layers.[S2]

c. Instrumentation

Electrochemical set-up: Electrochemical experiments were carried out using an Autolab potentiostat (PGSTAT 101) and a typical three-electrode configuration with a platinum mesh as counter electrode, an Ag/AgCl electrode (saturated KCl) as reference and the electrocatalysts as working electrode. A 0.1 M phosphate buffer (pH 7) was used as the electrolyte in all experiments. The measured values (vs Ag/AgCl) were then converted to potentials against the reversible hydrogen electrode (RHE) using the Nernst equation:

Equation S1. $V_{RHE} = V_{Ag/AgCl} + V_{Ag/AgCl}^{0} + 0.059 \cdot pH$

with $V_{Ag/AgCl}^{0}(saturated\ KCl) = 0.199\ V$

Spectroelectrochemical experiments: Spectroelectrochemistry (SEC), *i.e.* optical absorption as a function of applied potential, was measured by fitting the spectroelectrochemical cell in a Cary 60 UV-Vis spectrometer (Agilent Technologies). The measured data is generally presented as spectroelectrochemical difference spectra (ΔO.D.), which are generated by subtracting a reference spectrum (usually at the OCP or water-oxidation onset) from the absorption data obtained under

conditions of interest (e.g. higher applied potentials). The technique is explained in detail by Pastor et al.[4]

Step-Potential Spectroelectrochemistry (SP-SEC): We used this technique to estimate the extinction coefficient of the doubly oxidized species. This technique, has been reported by us previously,[S1] uses an electrochemical pump and an optical probe. The electrochemical pump (step-potential) is carried out by applying a squared (ON/OFF) voltage (potential difference) until steady-state conditions are reached. The effect of the applied potential on the electrocatalyst was monitored using light from a 100 W tungsten lamp, equipped with an Oriel cornerstone 130 monochromator. The transmitted probe light was filtered by several band pass and long pass filters (Comar Optics) and detected by a silicon photodiode (Hamamatsu S3071). Collected photons were converted to a voltage signal, sent to an amplifier (Costronics) and recorded by an oscilloscope (Tektronics TDS 2012c) and with a DAQ card (National Instruments, NI USB-6211) on the timescale of ms - s. Simultaneously, the extracted current was monitored using a Palmsense3 potentiostat. All data were acquired by a home-programmed LabView software.

Transient Absorbance Spectroscopy (TAS) The microsecond-second transient absorption decays were recorded using laser excitation pulses (6 ns) at 355 nm generated from a Nd:YAG laser (Big Sky Laser Technologies Ultra CFR Nd:YAG laser system, 6 ns pulse width, and 0.5 Hz). A liquid light guide with a diameter of 0.5 cm was used to transmit the laser pulse to the sample. The probe light source was a tungsten lamp (Bentham IL1 tungsten lamp), and the probe wavelength was selected using a monochromator (OBB-2001 dual grating, Photon Technology International) placed prior to the sample. Transient absorption data was collected with a Si photodiode (Hamamatsu S3071). The information was passed through an amplifier box (Costronics) and recorded using a Tektronics TDS 2012c oscilloscope (microsecond to millisecond timescale) and a DAQ card (National Instruments, USB-6211) (millisecond to second timescale). The data was processed using home-built software based on Labview. The decays observed are the average between 16 and 32 averages laser pulses.

As the area of the probed beam (0.28 cm^2) used to measure the change in the optical density was larger than the exposed area of the sample to the electrolyte, this was accounted for by dividing the raw data by the fractional area: $\frac{Area\ of\ sample\ exposed\ area}{Area\ of\ probed\ area}$.

Spectroelectrochemical Photo-Induced Absorption Spectroscopy (PIAS): Spectroelectrochemical Photo-induced absorption spectroscopy (PIAS) allows long-lived photogenerated species to be monitored under pseudo steady-state conditions. During these experiments, the sample was illuminated with light pulses (approximately 5 s on/5 s off), provided by a 365 nm LED (pump light). The change in absorbance was recorded using a probe light, which consisted of a tungsten lamp (Bentham IL1 tungsten lamp), and the probe wavelength was selected using a monochromator (OBB-2001, Photon Technology International) placed prior to the sample. Several long pass and band pass filters (Comar Instruments) were used to attenuate the pump light arriving at the detector. Transmitted photons were collected with a Si photodiode (Hamamatsu S3071). The signal was recorded with a DAQ card (National Instruments, USB-6211) without amplification.

As the area of the probed beam (0.28 cm^2) used to measure the change in the optical density was larger than the exposed area of the sample to the electrolyte, this was accounted for by dividing the raw data by the fractional area: $\frac{Area\ of\ sample\ exposed\ area}{Area\ of\ probed\ area}$.

A. Electrocatalyst activation process

The anodic electrodeposition methods used in this study produced FeOOH and Ni(Fe)OOH films. While FeOOH is stable in air, black NiOOH gradually changes to transparent $Ni(OH)_2$ in air when it is not anodically protected. Therefore, Ni(Fe)OOH and FeOOHNiOOH samples were activated before the optical and electrochemical experiments in order to convert $Ni(OH)_2$ in these samples to NiOOH. This process oxidises the $Ni^{II}(OH)_2$ to the higher valence NiOOH, leading to a strong absorption assigned to metal-to-oxygen charge transfer transition. To do this, the potential was swept from the open circuit potential of the sample to 1.5 V *vs.* the Ag/AgCl RE (scan rate = 10 mV/s) five times.[S1] The conversion of $Ni(OH)_2$ to NiOOH could be confirmed visually by the return of the black colour. The same activation procedure was also used for catalysts deposited on $BiVO_4$ photoanodes.

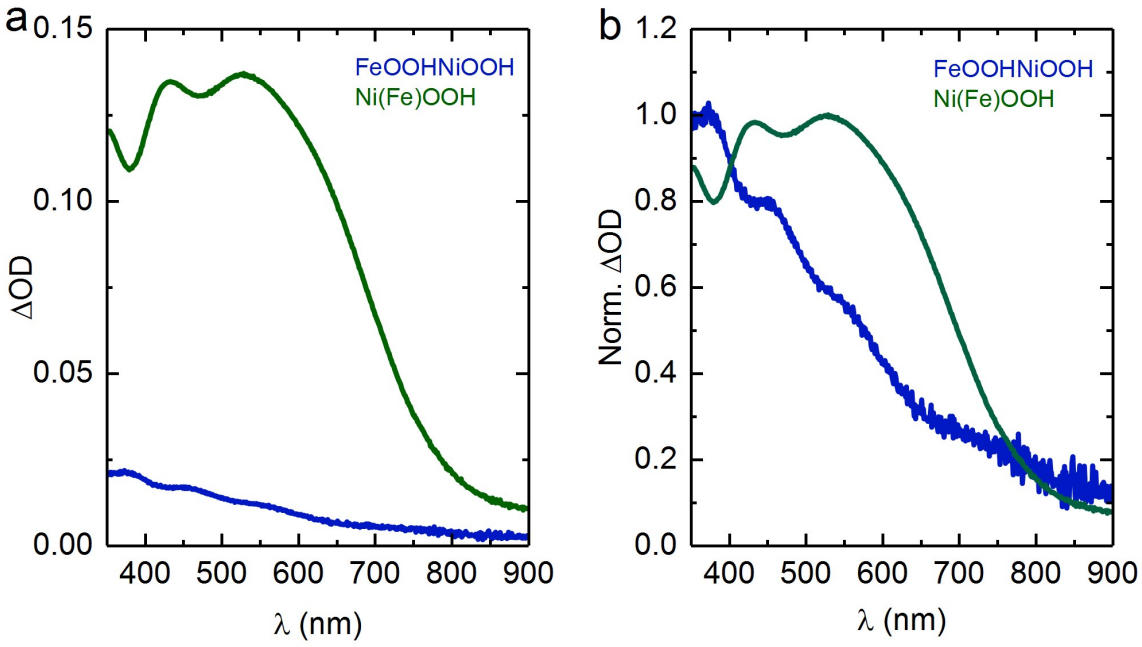

Figure S2. Spectra of MOOH(+) species after sample activation. (a) Differential UV-Vis absorbance spectra ($OD_{After\ activation} - OD_{Before\ activation}$) for Ni(Fe)OOH (green) and FeOOHNiOOH (blue); (b) Normalised ΔOD spectra.

B. SEC: Spectra of MOOH(++) species under electrochemical water oxidation

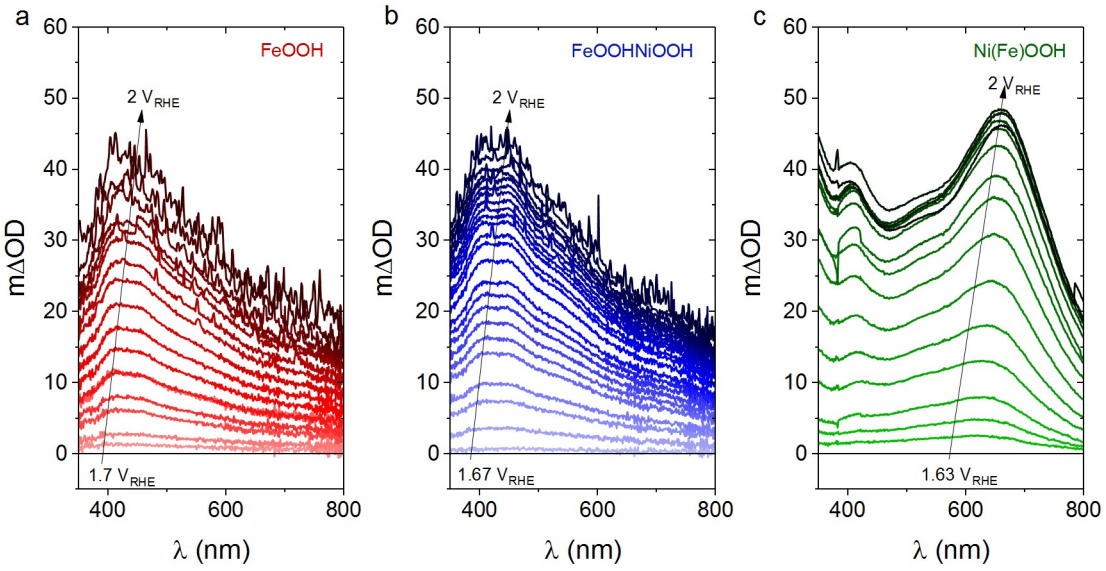

Figure S3. Differential UV-Vis spectra of the catalytic species at different applied potentials. The ΔOD was estimated by subtracting the absorbance at the catalytic onset from more positive applied potentials for (a) FeOOH, (b) FeOOHNiOOH and (c) Ni(Fe)OOH.

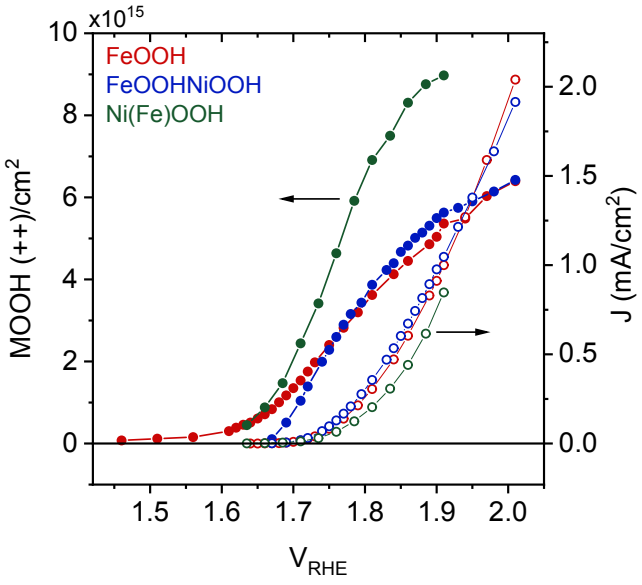

Figure S4. **Relationship between accumulated charge density (solid circles) observed optically and the applied potential.** The concomitant current density is plotted on the right axis (empty circles) for FeOOH (red), FeOOHNiOOH (blue) and Ni(Fe)OOH (green). Optical signals (ΔOD) were converted to MOOH(++)/cm^2 using extinction coefficients determined in section D.

C. NiOOH deactivation

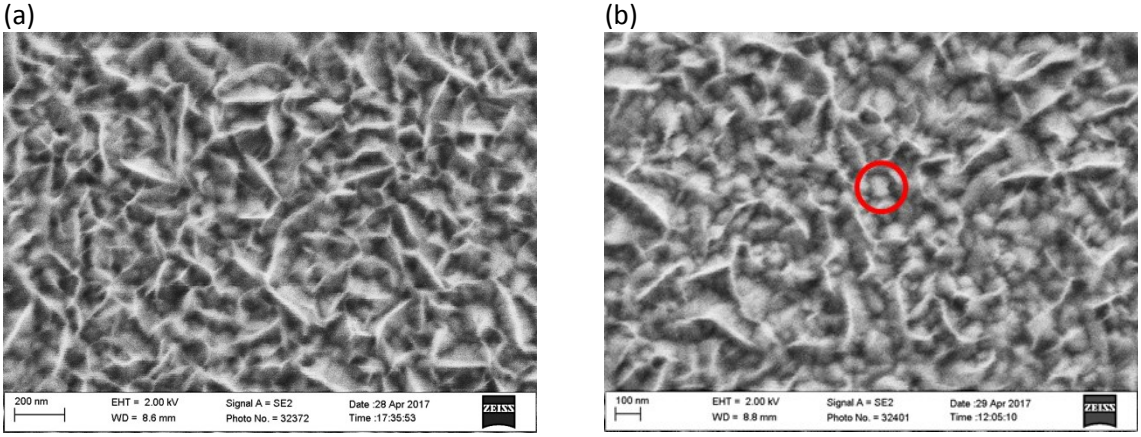

Figure S5. SEM images of a Ni(Fe)OOH (a) before and (b) after a bulk electrolysis of 2 h applying 2 V_{RHE}. The red circle indicates bare FTO observed after the experiment.

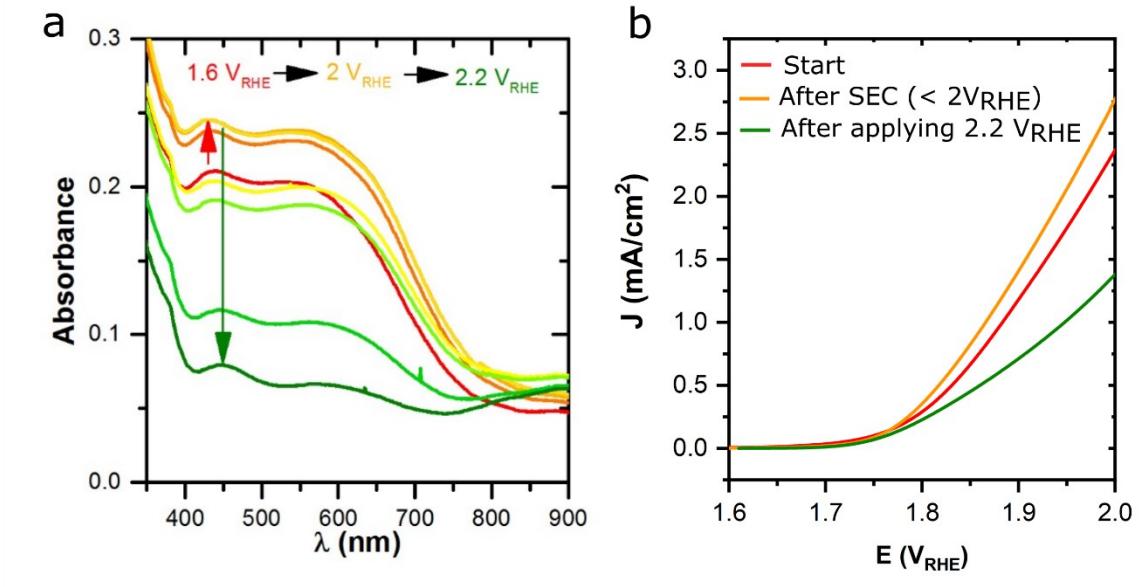

Figure S6. Degradation of Ni(Fe)OOH films at high applied potentials (> 2 V_{RHE}). (a) UV-Vis spectra from 1.6 V_{RHE} (red) to 2 V_{RHE} (yellow-orange) and to 2.2 V_{RHE} (green). (b) LSV before (red), after SEC experiments <2 V_{RHE} and after applying high positive potentials (orange) in the experiment shown in part (a).

D. *Extinction coefficient estimation*

The extinction coefficient of all the second oxidized species were estimated using the SP-SEC technique, reported previously.[S1] We monitored the changes in absorbance when a voltage step is applied. The recorded optical data is proportional to the population of the oxidized states at the applied potential (*Figures S7 a, c, e*). Simultaneously, the corresponding current is measured with an increase of current at the high applied potential and a reductive spike once the potential is turned to a lower one. The latter corresponds to the reduction of the accumulated oxidized states at the high potential region. The integration of these reductive currents allow us to quantify the electrons used to reduce the oxidized states. Using the Lambert-Beer law (*Equation S2*) we can estimate the corresponding extinction coefficients by plotting ΔOD against the electrons extracted (Figures S7 b, d, f). The slope of the corresponding graphs yields the Ɛ in cm^2/number of e^-, which can be transformed to $M^{-1}\,cm^{-1}$ as detailed:

Equation S2 $A = \varepsilon \times c$ where A = Absorbance at a particular wavelength, Ɛ is the extinction coefficient and c is the concentration in electrons per cm^2.

$$5.8 \times 10^{-18} \frac{cm^2}{no\ of\ e^-} \times \frac{6.022 \times 10^{23}\ no\ of\ e^-}{1\ mol\ e^-} \times \frac{1\ dm^3}{1000\ cm^3} = 3500\ M^{-1} cm^{-1}$$

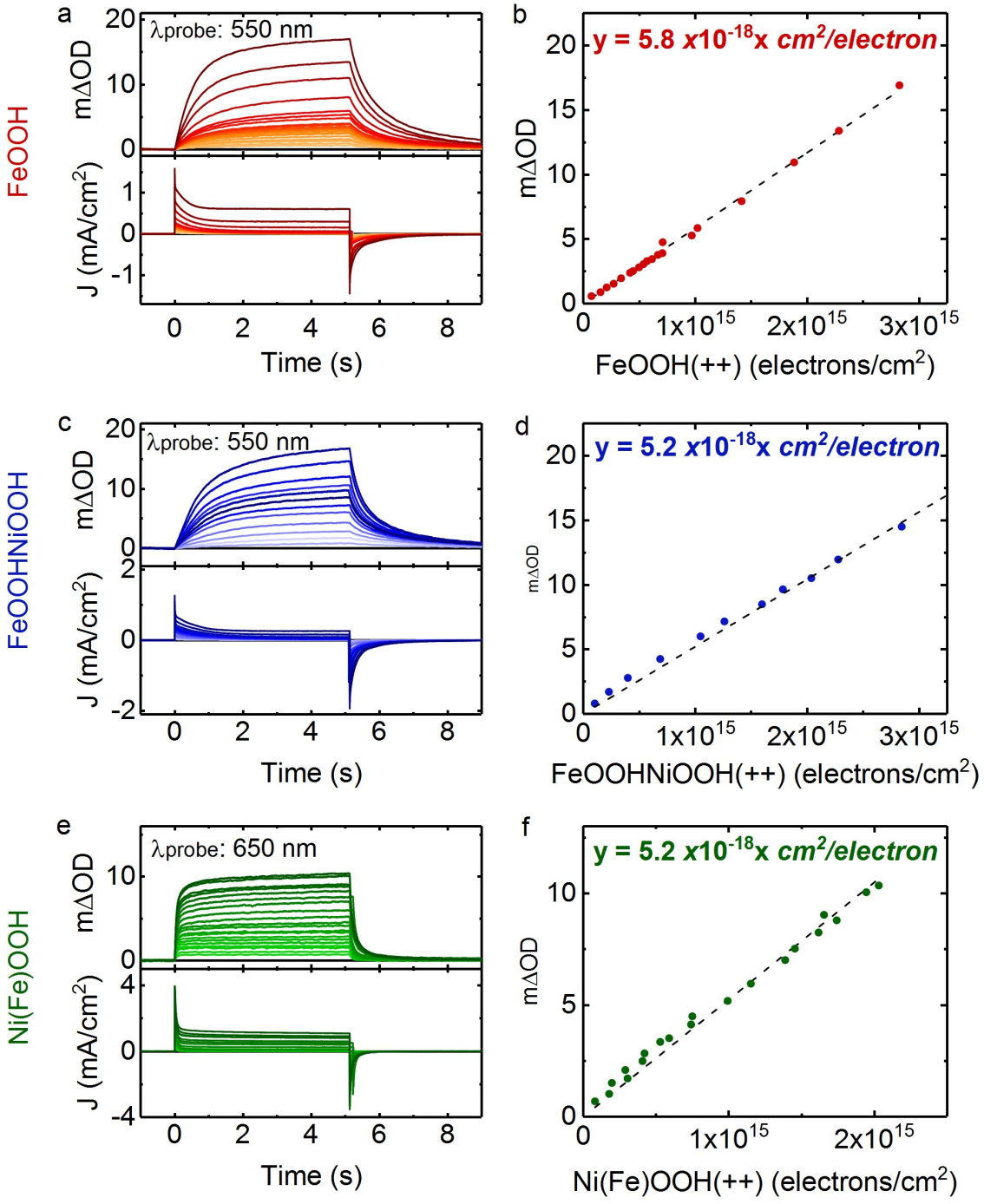

Figure S7. SP-SEC of electrocatalysts to estimate the extinction coefficients of MOOH(++) species. (a) SP-SEC for FeOOH from 1.72 V_{RHE} to the desired potential (up to 1.91 V_{RHE}) where the top panel shows the optical data at 550 nm, and the bottom panel shows the current density. (b) Plot of the optical signal at 550 nm against the charge density. (c) SP-SEC for FeOOHNiOOH from 1.64 V_{RHE} to the desired potential (up to 1.81 V_{RHE}) where the top panel shows the optical data at 550 nm, and the bottom panel shows the current density. (d) Plot of the optical signal at 550 nm against the charge density. (e) SP-SEC for Ni(Fe)OOH from 1.72 V_{RHE} to the desired potential (up to 1.91 V_{RHE}) where the top panel shows the optical data at 650 nm, and the bottom panel shows the current density. (f) Plot of the optical signal at 650 nm against the charge density.

E. Transient absorption spectroscopy

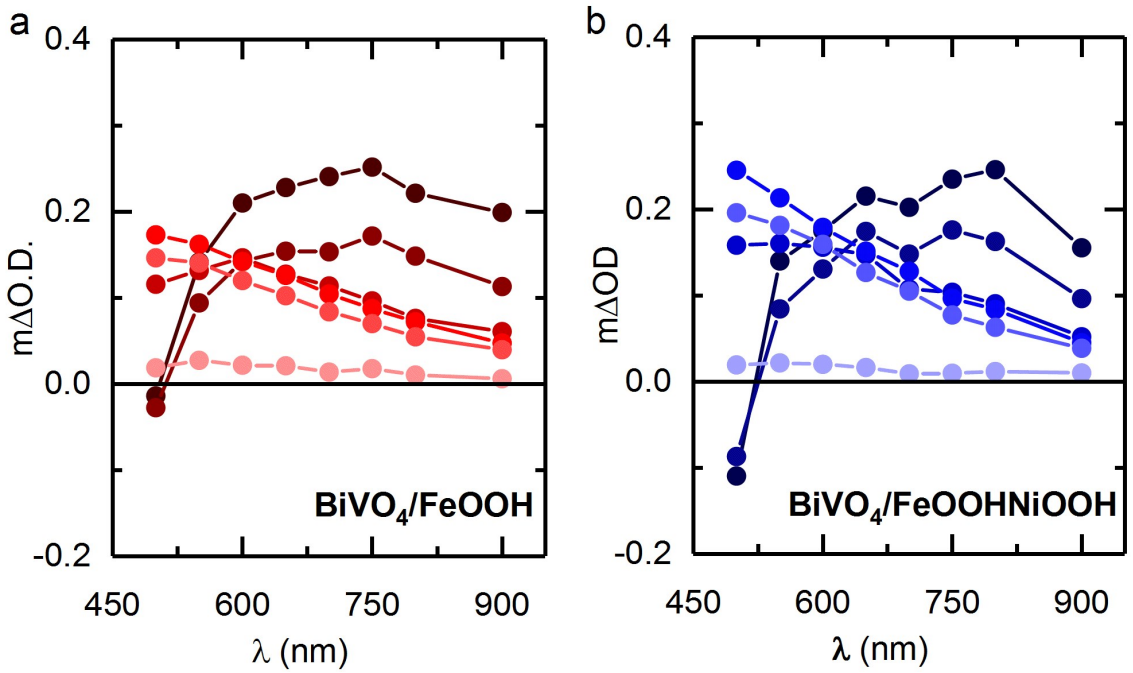

Figure S8. Transient absorption spectra (dark to light colours representing spectra at 10 µs – 100 µs – 1 ms – 10 ms – 100 ms – 1 s) of (a) $BiVO_4$/FeOOH and (b) $BiVO_4$/FeOOHNiOOH. All measurements were obtained under 1.4 V_{RHE} applied bias, at pH7. The samples were excited at 355 nm (300 µJ cm^{-2}).

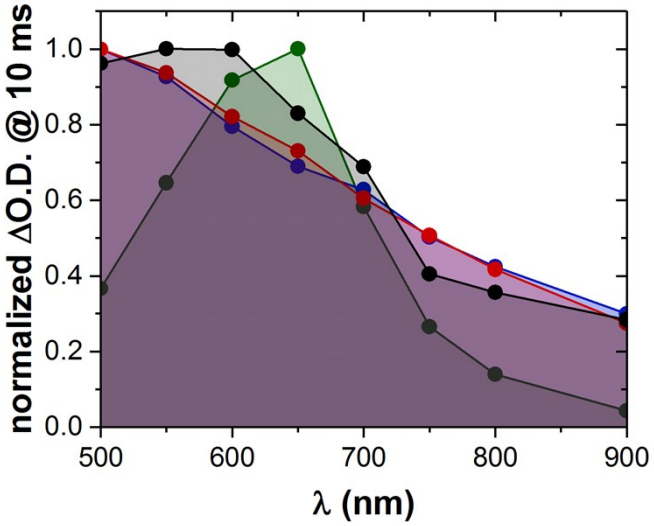

Figure S9. Normalised TA spectra at 10 ms for $BiVO_4$ (black), $BiVO_4$/FeOOH (red), $BiVO_4$/FeOOHNiOOH (blue) and $BiVO_4$/Ni(Fe)OOH (green).

F. Stability of $BiVO_4$/Ni(Fe)OOH photoanodes

(a) (b)

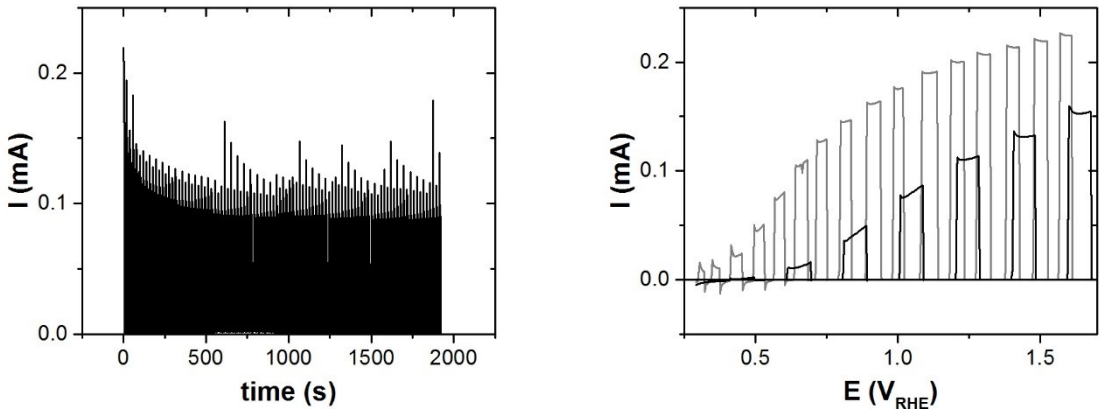

Figure S10. Stability of $BiVO_4$/Ni(Fe)OOH. (a) Chopped chronoamperometry under 1 sun at 1.41 V_{RHE} and (b) chopped LSV under 1 sun before (grey) and after (black) the chronoamperometry presented in Figure S5a.

G. TOF (s^{-1}) and τ (s) calculation from measured [++] state densities and electrochemically measured water oxidation current densities.

In order to calculate these parameters, we need the number of accumulated [++] (cm^{-2}), which are derived from the conversion of the obtained ΔOD using the extinction coefficient. On the other hand, the current density data (A/cm^2) can be transformed into number of electrons/s using the electron charge (1.60 x 10^{-19} Coulombs).

For TOF calculation we consider that to produce one molecule of oxygen 4 oxidized species are needed:

Equation S3. $$TOF\left(s^{-1}\right) = \frac{number\ of\ electrons\ \times\ s^{-1}}{4\,[\,++\,]}$$

τ is the lifetime of the oxidized species MOOH(++):

Equation S4. $$\tau\,(s) = \frac{[\,++\,]}{number\ of\ electrons\ \times\ s^{-1}}$$

References

S1 L. Francàs, S. Corby, S. Selim, D. Lee, C. A. Mesa, R. Godin, E. Pastor, I. E. L. Stephens, K.-S. Choi and J. R. Durrant, *Nat. Commun.*, 2019, **10**, 5208.

S2 T. W. Kim and K.-S. Choi, *Science (80-.).*, 2014, **343**, 990–994.

S3 S. Zou, M. S. Burke, M. G. Kast, J. Fan, N. Danilovic and S. W. Boettcher, *Chem. Mater.*, 2015, **27**, 8011–8020.

S4 E. Pastor, F. Le Formal, M. T. Mayer, S. D. Tilley, L. Francàs, C. A. Mesa, M. Grätzel and J. R. Durrant, *Nat. Commun.*, 2017, **8**, 14280.